Geophysical Research Letters

RESEARCH LETTER
10.1029/2023GL103322

Contributions of Climate Change and ENSO Variability to Future Precipitation Extremes Over California

Xingying Huang[1] and **Samantha Stevenson**[2]

[1]National Center for Atmospheric Research, Boulder, CO, USA, [2]Bren School of Environmental Science and Management, University of California, Santa Barbara, CA, USA

Key Points:

- The contributions from El Niño/Southern Oscillation (ENSO)-driven SST variability to extreme precipitation are quantified using multiple model ensembles and Coupled Model Intercomparison Project Phase 5 data
- The effect of ENSO variability is comparable to or even larger than the overall impact from climate change for extreme precipitation events
- Better constraining ENSO-related SSTA patterns and associated teleconnections is necessary for more accurate precipitation extremes changes

Supporting Information:

Supporting Information may be found in the online version of this article.

Correspondence to:

X. Huang,
xingyhuang@gmail.com

Citation:

Huang, X., & Stevenson, S. (2023). Contributions of climate change and ENSO variability to future precipitation extremes over California. *Geophysical Research Letters*, *50*, e2023GL103322. https://doi.org/10.1029/2023GL103322

Received 24 FEB 2023
Accepted 23 MAY 2023

Author Contributions:

Conceptualization: Xingying Huang, Samantha Stevenson
Data curation: Xingying Huang
Formal analysis: Xingying Huang
Funding acquisition: Samantha Stevenson
Investigation: Xingying Huang
Methodology: Xingying Huang, Samantha Stevenson

Abstract The El Niño/Southern Oscillation (ENSO) affects the occurrence frequency and intensity of extreme precipitation through modulations of regional heat and moisture fluxes. California experiences particularly strong ENSO influences and models project different to its extreme precipitation. It remains unclear how diverse projections of future precipitation extremes relate to inter-model differences for those changing signals. Here, we use "large ensemble" simulations with multiple climate models along with the Coupled Model Intercomparison Project Phase 5 to investigate the range of precipitation extreme changes over California and the influences from ENSO-related teleconnections. We found that precipitation amount increases are much larger during El Niño relative to La Niña years, mainly caused by the differences in frequency of extreme events during different phases. The ENSO-driven effect is even larger than the overall climate change signal for the most extreme events, implying uncertainties from inter-model differences in ENSO-related SST variability for extreme precipitation changes.

Plain Language Summary Regional projected precipitation changes over California are associated with large uncertainties due to both climate variabilities, external forcing, and model internal uncertainties. Extreme precipitation in California is projected to intensify, and how mean-state climate change and El Niño/Southern Oscillation (ENSO)-related SST variability contribute to different changes are focused on with a set of "large ensemble" simulations. Precipitation extremes, as a significant topic for climate impacts, are focused in this study for future changes and distributions within models' large ensemble. We found that the effect of ENSO variability is comparable to the magnitude of overall future changes and even larger than mean climate impacts for the most precipitation extreme events. Projections of future precipitation extremes are diagnosed for the influences from changes to ENSO variability with mean-state forcings.

1. Introduction

Large-scale climate variability, such as the El Niño/Southern Oscillation (ENSO), has impacts on extreme events around the world. California is a particularly vulnerable region, experiencing significant impacts due to extreme precipitation including but not limited to water resources and flood management (Huang, Stevenson, & Hall, 2020; Oakley et al., 2018; White et al., 2019). Cayan et al. (1999) showed that in El Niño years, extremes (exceeding the 90th percentile) in daily precipitation and streamflow are more frequent over the Southwest and are less frequent during La Niña years, based on daily historical data over the western United States. Jong et al. (2016) examined El Niño's impacts on California winter precipitation, using observational data from 1901 to 2010 and found that the El Niño influence on California precipitation strengthens from early to late winter and is stronger in the southern portion of the state.

As climate change progresses, precipitation extremes are generally projected to intensify due to changes in atmospheric thermodynamics (Huang & Stevenson, 2021; Huang, Swain, & Hall, 2020; O'Gorman & Schneider, 2009; Pendergrass & Hartmann, 2014; Pfahl et al., 2017). These hydrological extremes over the US west coast are mainly associated with atmospheric rivers (ARs), especially for the strongest events (Dettinger, 2013; Dettinger et al., 2011; Huang & Swain, 2022; Ralph et al., 2004; Zhu & Newell, 1998). Previous studies (e.g., Payne & Magnusdottir, 2014) have shown the role of ENSO in modulating landfalling ARs over the US west coast using MERRA reanalysis data, with more frequent AR occurrences during the El Niño phase relative to La Niña. Given ENSO's influences on the trajectory of ARs (Hoell et al., 2016; Payne & Magnusdottir, 2014; Schubert et al., 2008), the relationship of ENSO with future projected changes in precipitation extremes is an important consideration. However, the influence of projected future climate change on ENSO-related SST variability is

Project Administration: Samantha Stevenson
Resources: Xingying Huang
Software: Xingying Huang
Supervision: Samantha Stevenson
Validation: Xingying Huang
Visualization: Xingying Huang
Writing – original draft: Xingying Huang
Writing – review & editing: Xingying Huang, Samantha Stevenson

unclear, as climate models disagree on the magnitude and direction of the projected changes to overall SST variance (Bellenger et al., 2014; Fredriksen et al., 2020; Maher et al., 2022; Stevenson, 2012).

One of the missing ingredients is to look directly at how changes to future precipitation extremes are related to ENSO, mean Pacific climate, and inter-model structural differences, which is the aim of the present study. This is enabled by the recent increase in popularity of "large ensembles," suites of many (~20–100) simulations run with the same climate model under varying initial conditions. Here we investigate the features of precipitation extreme changes over the California region by examining results from the Multi-Model Large Ensemble Archive (MMLEA; Deser et al., 2020). In addition, we have retrieved a selection of global climate models (GCMs) from the Coupled Model Intercomparison Project Phase 5 (CMIP5) (Taylor et al., 2012) to comprehensively analyze ENSO-related variability and uncertainties in future precipitation extremes, by considering both inter-model differences and internal variability within model ensembles. We focus on extreme precipitation and its response to climate change at a state-wide scale, to illustrate how models' representation of ENSO pattern and amplitude interplays with precipitation extremes under a changing climate.

2. Methods and Data Sets

Much of the data used in this study is derived from the Multi-model Large Ensemble Archive (see Table S1 in Supporting Information S1) (Deser et al., 2020), compiled at the National Center for Atmospheric Research and containing multiple realizations of 20th and 21st century simulations for several different GCMs. In our analyses, the "historical" period refers to 1951–2000, and the "future" period refers to 2051–2100 under RCP8.5 (a high-emission scenario). Selected MMLEA models are used here according to the availability of all variables needed in this work, for which CESM1, CSIRO-Mk3.6, GFDL-CM3, and CanESM2 provided output (see Table S1 in Supporting Information S1 for details).

In addition to the MMLEA, we have retrieved a set of CMIP5 models (see Table S2 in Supporting Information S1). Although the CMIP5 models generally do not provide many ensemble members per model, the inclusion of many different models allows a more comprehensive look at inter-model differences in ENSO variability and climate change influences, which complements the smaller model set but larger ensemble sizes provided by the MMLEA.

Daily precipitation (Pr) is used to identify precipitation extremes, defined as the state-mean intensity exceeding the 99th percentile for each time period (i.e., 1951–2000 and 2051–2100 respectively). This calculation is based on all the daily Pr values masked over the California region for each ensemble member. Extreme precipitation is defined as days exceeding the 99th percentile of the distribution over the relevant period. We acknowledge that ENSO effects could behave differently for different regions of California (such as northern CA vs. southern CA) (e.g., as discussed in Hoell et al., 2016; Payne & Magnusdottir, 2014), which we will only focus on the whole California region considering the overall coarse resolution and does not classify ENSO intensity into different categories in this study. For the analyses of models' mean, we have regridded all the data set to 1°.

For the calculation of SST (surface sea temperature) and SLP (sea level pressure) anomalies, the relevant variables are detrended after the seasonal cycle is removed. The Niño 3.4 SST anomaly is the SST anomaly over the Niño 3.4 region ([5N–5S, 120–170W]) (https://www.ncdc.noaa.gov/teleconnections/enso/indicators/sst/, NOAA) calculated based on the detrended monthly SST data. El Niño/La Niña years are defined as the years when the DJF-average Niño 3.4 index exceeding ±1 of the standard deviation (Okumura & Deser, 2010), where the Niño 3.4 index (monthly) is based on the 3-month running means of SST anomalies in the Niño 3.4 region relative to the 30-year running mean.

3. Results

3.1. Future Changes in Mean and Extreme Precipitation

First, we investigated the model representation of ENSO and its impacts on CA precipitation. For simulated historical precipitation, we found that the mean precipitation over the historical period (1951–2000) for state average as investigated here is ~1.9 mm/day for the MMLEA and ~2.2 mm/day for CMIP5, close to the CPC (Unified Gauge-Based Analysis of Daily Precipitation) (relatively fine-resolution, 0.25 × 0.25°) observational mean value of ~1.6 mm/day and NCEP (National Centers for Environmental Prediction) (atmospheric reanalysis,

10.1029/2023GL103322

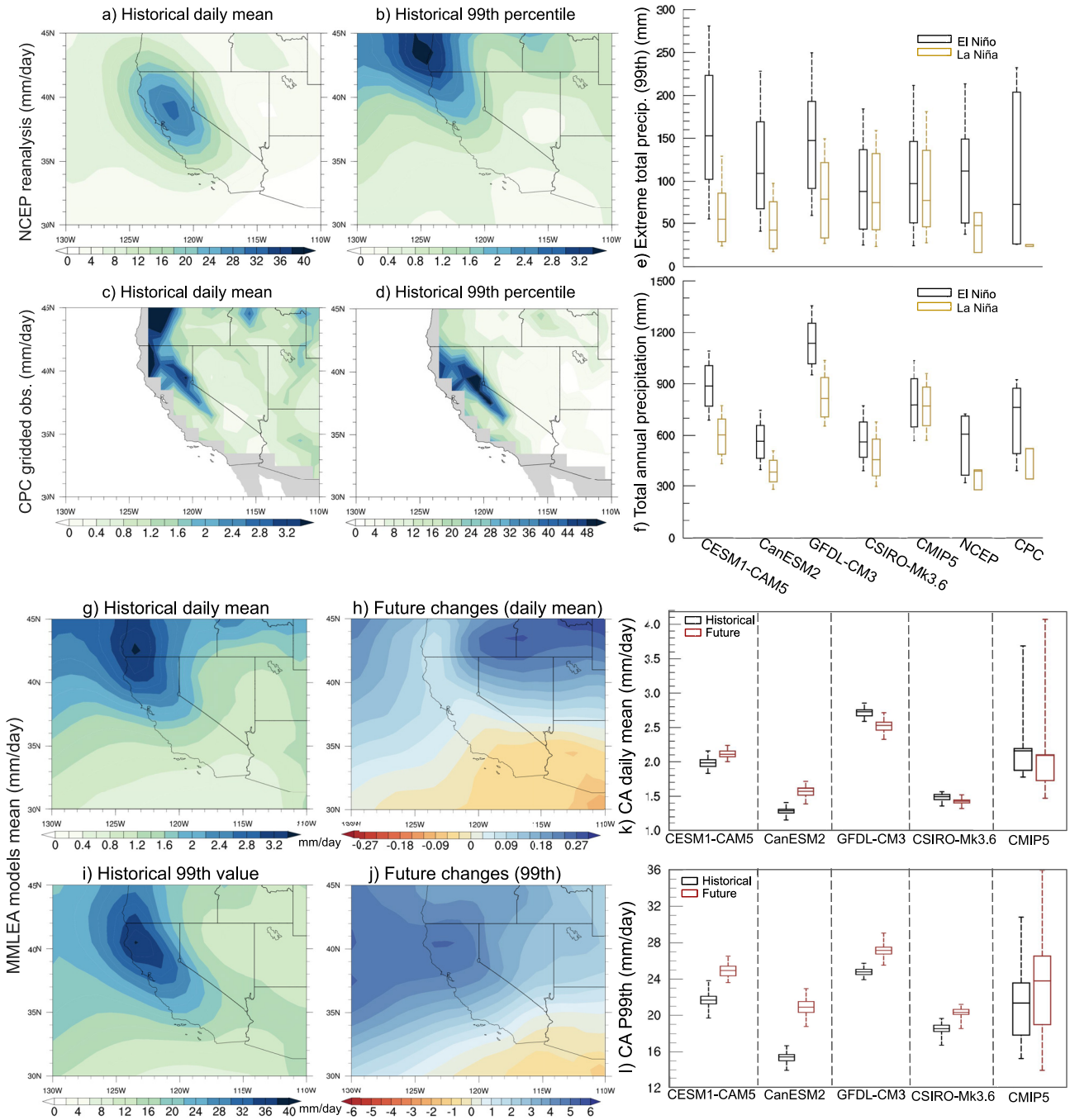

Figure 1. Top: mean and extreme precipitation from the NCEP reanalysis (a and b) and CPC observation data (c and d) over 1951–2000, and El Niño/Southern Oscillation effect on California precipitation: boxplot of (e) extreme precipitation and (f) mean precipitation. (Here, the boxplot represents the values for 1/8th, 25th, medium, 75th, and 7/8th from lower to top whiskers based on the state-average values.); Bottom: mean and extreme precipitation and their future changes in the MMLEA and Coupled Model Intercomparison Project Phase 5 (CMIP5). (g and h) Historical daily mean precipitation (i.e., total precipitation divided by the number of days over all years from daily data) and its future change averaged over the four MMLEA ensembles; (i and j) Historical extreme precipitation and its future changes; (k and l) Boxplot of the ensemble spread (among all members in MMLEA and all CMIP5 model members) in CA precipitation, in terms of daily mean (k) and 99th percentile (l). The 99th percentile is determined from state-mean values (Here the box width corresponds to the interquartile range, and whiskers indicate the maximum and minimum value in the relevant ensemble).

coarse resolution, 2.5 × 2.5°, closer to the GCMs' grid spacings) mean value of ∼1.2 mm/day (Figures 1a–1d, and 1g). For the extreme precipitation mean, the MMLEA value is ∼25.5 mm/day and CMIP5 ∼26.7 mm/day, which is close to the CPC observational mean (about 23.7 mm/day) but larger than the NCEP reanalysis value of 18.6 mm/day.

We have also examined models' capacity to represent the ENSO effect on California precipitation over the historical period (Figures 1e–1f). The effects of ENSO on both mean and extreme precipitation are examined by separating El Nino and La Nina phases in the MMLEA ensembles, CMIP5 models, and NCEP observations. The results show that the ENSO effect is important for both California's total annual precipitation amount and the magnitude of extreme precipitation events, as seen in NCEP and most of the MMLEA ensembles (except for the CSIRO-Mk3.6 model, which shows a relatively weak ENSO effect). However, the ENSO signal is less clear when the CMIP5 models are considered as a whole (Figure 1), with both the mean and extreme precipitation being similar across El Nino and La Nina years. This is most likely due to models with very different ENSO teleconnection structures being averaged together, blurring the signal in the ensemble mean.

We analyze the changes to mean and extreme precipitation characteristics (Figure 1) between the historical and future periods for MMLEA and CMIP5 data. When comparing historical precipitation behavior across models (Figure 1k), it is obvious that there is a large range in model representation of historical precipitation, with MMLEA ensemble means ranging from ∼1.3 to 2.7 mm/day (Figure 1k, black boxes). When the full suite of CMIP5 models is considered, the range of inter-model differences is even larger (Figure S3 in Supporting Information S1). This is likely caused in part by known differences in simulated mean North Pacific circulation (Huang & Stevenson, 2021), different magnitudes of internal variability, as well as differences in model representations of physical processes (Rupp et al., 2013) and models variability in midlatitude circulation patterns that exist within CMIP5 (Simpson et al., 2014). Models also generally capture the spatial structure of precipitation of California, with higher values of both mean and extreme precipitation overall in northern California compared to the southern part of the state (Figures 1b, 1d, 1g, and 1h). We expect that orographic influences are underestimated relative to observations but identifying the magnitude of this effect is beyond the scope of this study.

The magnitude of future changes to mean precipitation are inconsistent among the models, with CESM1 and CanESM2 showing an overall state-wide increasing trend, but there is a decreasing trend in the GFDL-CM3 and CSIRO-Mk3.6 (Figure 1k). Ensemble spread can be substantial as well, as illustrated by the relatively large spread across realizations from a single GCM (Figure 1k); however, in all four large ensembles, the difference between the historical and future distributions of mean precipitation is statistically significant. The CMIP5 mean shows a slight reduction in mean precipitation, although again the CMIP5 inter-model spread is larger than the spread between the MMLEA ensembles (Figure 1k; also see Figure S3 in Supporting Information S1). This apparent lack of signal is a result of the CMIP5 ensemble mean including a wide range of model behaviors (cf. the diversity of signatures in the MMLEA models alone); further demonstration of this is illustrated by the distributions of historical and future precipitation in the individual CMIP5 models used in this analysis (Figures S3e and S3f in Supporting Information S1).

Uncertainty in the simulated magnitude of extreme precipitation over the historical period is also apparent among models, with the historical ensemble mean 99th percentile value ranging from ∼15 to 25 mm/day (Figure 1l). However, the effect of climate change is consistent in its direction; there is a significant increasing trend in the future period across the ensemble mean in all of the different MMLEA ensembles. The 99th percentile value also increases modestly in CMIP5 mean (Figure 1l), although the signal is not as strong as in the MMLEA ensemble mean. The magnitude of the future intensification does differ, with increases ranging from about 10% to 35% in the MMLEA.

To understand the large-scale climate anomaly patterns underlying the extreme precipitation over California, we further investigate the SST and SLP patterns over the tropical and north Pacific regions (Figure 2) during extreme precipitation days. The data is detrended to remove the seasonal cycle and the anthropologic warming trend. The anomaly patterns associated with extreme precipitation days show some differences across model ensembles, in both SST and SLP, likely relates to the differences in ENSO amplitude across models (Figures S1 and S2 in Supporting Information S1). However, in general, there is a tendency in all models (both MMLEA and CMIP5) for extreme precipitation days to be associated with "El Niño-like" anomaly patterns based on the composite SST anomaly (Figure 2a) over the historical period, which is also present in the NCEP reanalysis and CMIP5 mean (Figure S4 in Supporting Information S1). There is an overall warming band over the subtropical to southern coastal ocean off California (Figure 2a) which indicates the southward movement of midlatitude moisture tracks carrying concentrated vapor inflows during extreme precipitation events (Huang & Stevenson, 2021).

10.1029/2023GL103322

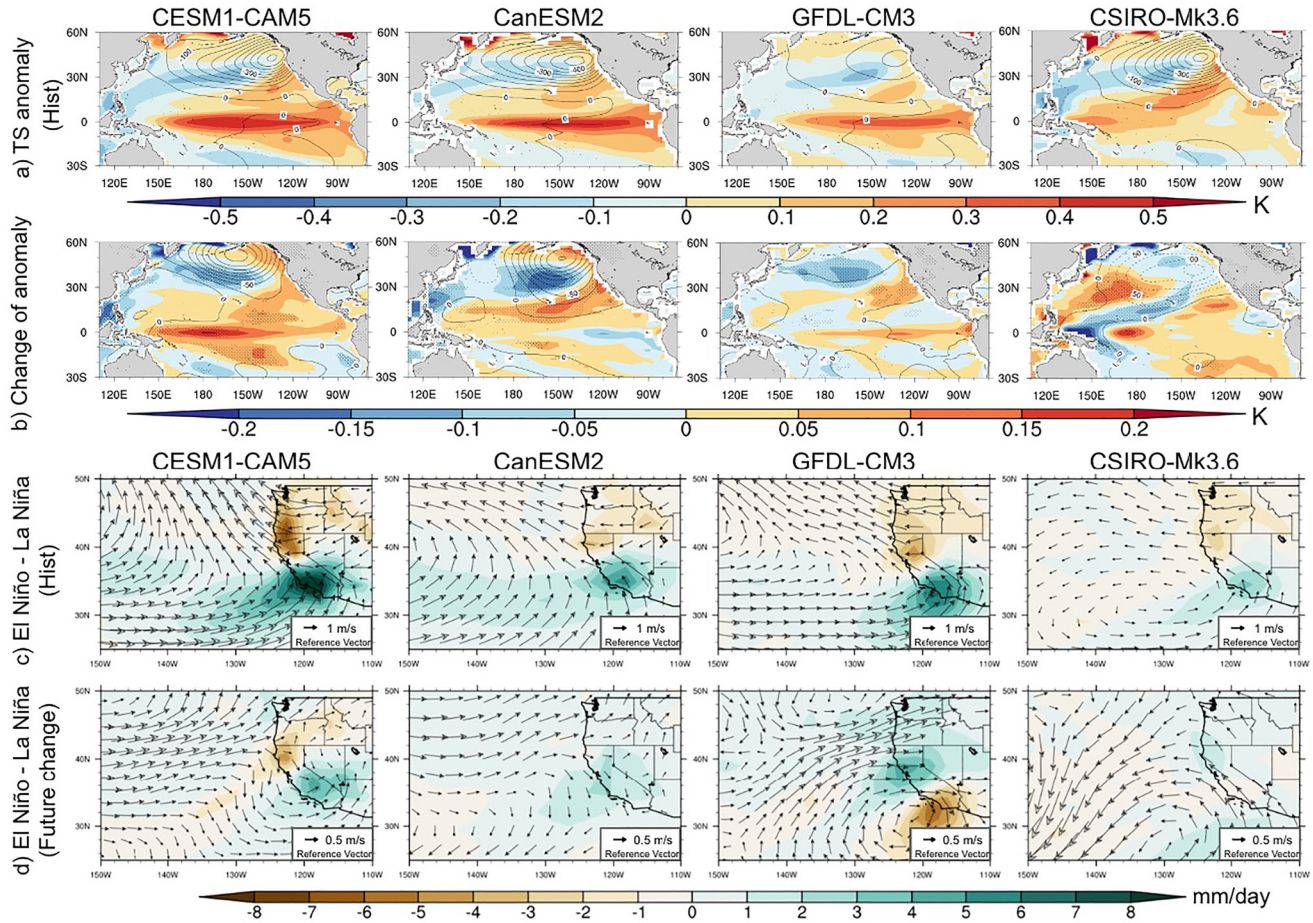

Figure 2. Panels (a and b): SST (colors) and SLP (contours) anomaly (detrended for each model at each month) for extreme precipitation days. (a) Ensemble mean SST (colors) and SLP (contours) (note that solid contours indicating negative values, and dotted ones for positive values) anomalies over the historical period with detrended values for each model; (b) as in (a), but for future changes of the anomaly (stippled areas refer to the regions where more than 80% of the ensemble members agree on the sign of the SST change). Panels (c and d): Ensemble mean difference pattern between El Niño and La Niña for historical extreme precipitation intensity over CA and future changes for each model. We calculated the mean extreme precipitation intensity and the average near-surface winds for the days during El Niño and La Niña phases in each time period for each member of the MMLEA models, then computed the ensemble mean. (c) Difference of the mean extreme precipitation intensity and the average near-surface winds between El Niño and La Niña conditions for the historical period; (d) Difference between the (El Niño—La Niña) precipitation and near-surface winds, differenced between the future and historical periods. (Winds at the 850 hPa level for all models except CanESM2, where 10 m wind is used given the data availability).

Future changes in the SST and SLP anomaly patterns associated with extreme precipitation days also differ among the models (Figure 2b). In CESM1 and GFDL-CM3 there is increased warming along the equatorial Pacific during extreme precipitation days, whereas this warming is less pronounced in CSIRO-Mk3.6 and nearly absent in CanESM2. The behavior of the NINO3.4 time series (see Figure S5 in Supporting Information S1) also differs in these models, with CESM1-CAM5 showing an increasing trend, CanESM2 showing a decreasing trend, and GFDL-CM3 showing nonmonotonic behavior with variance peaking near 2020, while CSIRO-Mk3.6 exhibits a relatively stable state before the late 21 century.

The teleconnection effects from ENSO variability are further illustrated in Figures 2c and 2d. The extreme precipitation intensity for El Nino is calculated as the mean precipitation for all the extreme precipitation days during El Nino years, and the equivalent calculation is also performed for La Nina years. Figure 2c demonstrates that El Nino years generally favor a dipolar pattern in precipitation extremes, with increased precipitation in southern California and decreases in the northern portion of the state. This is consistent with the known tendency for the midlatitude jet and AR landfalls to shift southward during El Nino events (Payne & Magnusdottir, 2014). This dipolar pattern becomes more pronounced in the future in the CESM1, and to a lesser extent in CanESM2 (Figure 2d). However, the other two MMLEA ensembles behave differently: little change is observed in CSIRO-Mk3.6, and in GFDL-CM3, the future changes tend toward weakening of the dipolar pattern.

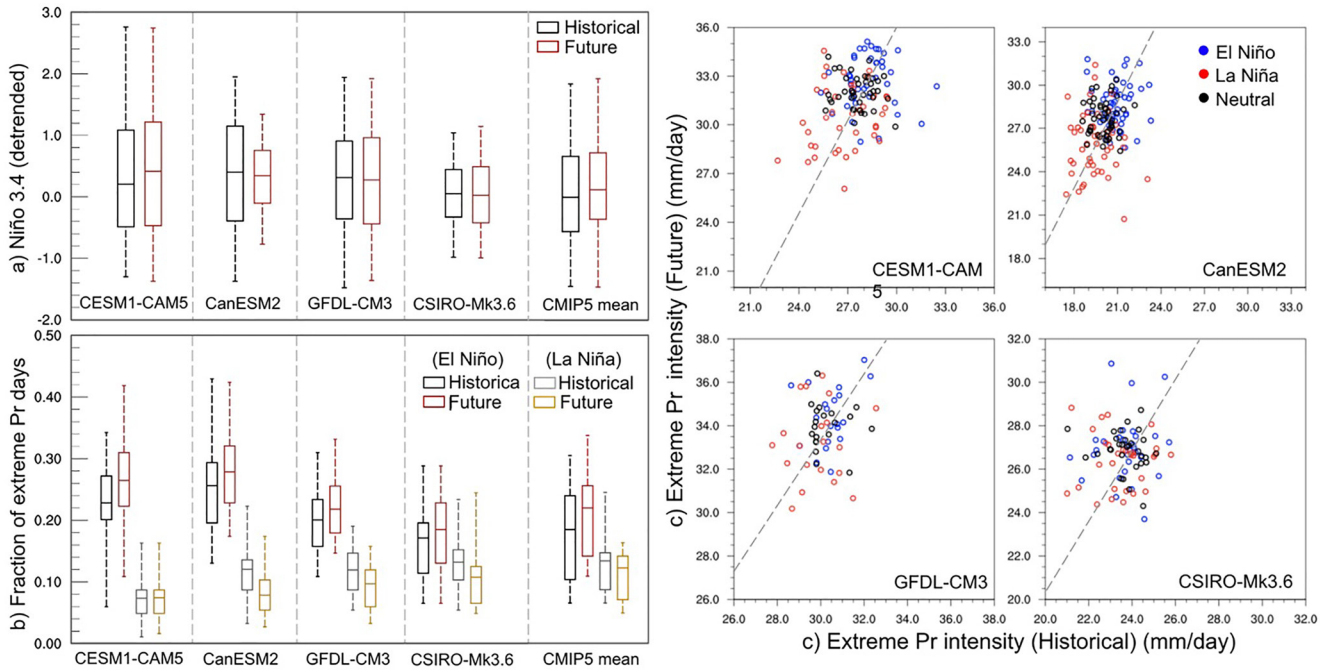

Figure 3. El Niño/Southern Oscillation (ENSO) influences on precipitation extremes, expressed as frequency and intensity changes. (a) Boxplot of Niño 3.4 DJF SST anomaly during extreme precipitation days for all ensemble members of each model and Coupled Model Intercomparison Project Phase 5 collection (here, the interval between the lower and top whiskers indicates the 90% confidence interval, and the box width represents the interquartile range); (b) Boxplot of fraction of extreme precipitation days occurring during El Niño and La Niña years; (c) Scatter plot of the mean extreme precipitation intensity at different phases of ENSO for each ensemble member.

3.2. ENSO Influences on Precipitation Extremes

We further investigate how ENSO and its teleconnections affect the future behavior of precipitation extremes. To understand this relationship, we first use the Niño 3.4 index to quantify ENSO variability during extreme precipitation days (Figure 3a) for MMLEA models, averaging all the ENSO phrases including neutral state. We acknowledge that the average Niño 3.4 index values are not particularly aimed to identify the strength of El Niño versus La Niña but for the overall representation of ENSO variability, indicating the models are intrinsically different for simulating ENSO amplitude. The models used here differ in their projections of future ENSO amplitude, consistent with previous analyses of both CMIP5 and CMIP6-era model behavior (Bellenger et al., 2014; Fredriksen et al., 2020; Maher et al., 2022; Stevenson, 2012). In the MMLEA, the CESM1 is the only model showing significant ENSO strengthening, and CanESM2 the only model where ENSO weakens significantly (see Figure S5 in Supporting Information S1). The CMIP5 likewise is roughly evenly split on the direction of ENSO amplitude changes (Bellenger et al., 2014; Stevenson, 2012; Stevenson et al., 2021) with the mean blurring together models with very different behaviors.

Despite the differences in projected ENSO amplitude across models, there appear to be some consistent changes in the impact of ENSO on future precipitation extremes. Even in the historical climate, models simulate an enhanced frequency of extreme precipitation days during El Niño years relative to La Niña, consistent with what is observed in the real world (Figures S6 and S7 in Supporting Information S1). This fraction of extreme precipitation days occurring during El Nino years increases in the future for all models (Figure 3b), with increases ranging from about 8% to 16% for the MMLEA (and most pronounced for CESM1). We have also clarified that it is not referring that El Niño events are increasing but the ENSO influences on precipitation extremes. Further, precipitation extremes are predicted to be nearly the same or less frequent during La Niña years in all models (Figure 3b, Figure S7 in Supporting Information S1).

Using this analysis, we can quantify how the effect of ENSO compares with the effect of anthropogenic forcing, which is known to be robustly projected to increase the frequency of precipitation extremes overall (Pfahl et al., 2017). For instance, in CESM1 and CanESM2 (Figure 3c; Figure S8 in Supporting Information S1) the differences between the ensemble mean of El Niño and La Niña-associated precipitation extremes are comparable to the differences between historical and future mean values. However, in CSIRO-Mk3.6, the ENSO effect on the extreme precipitation

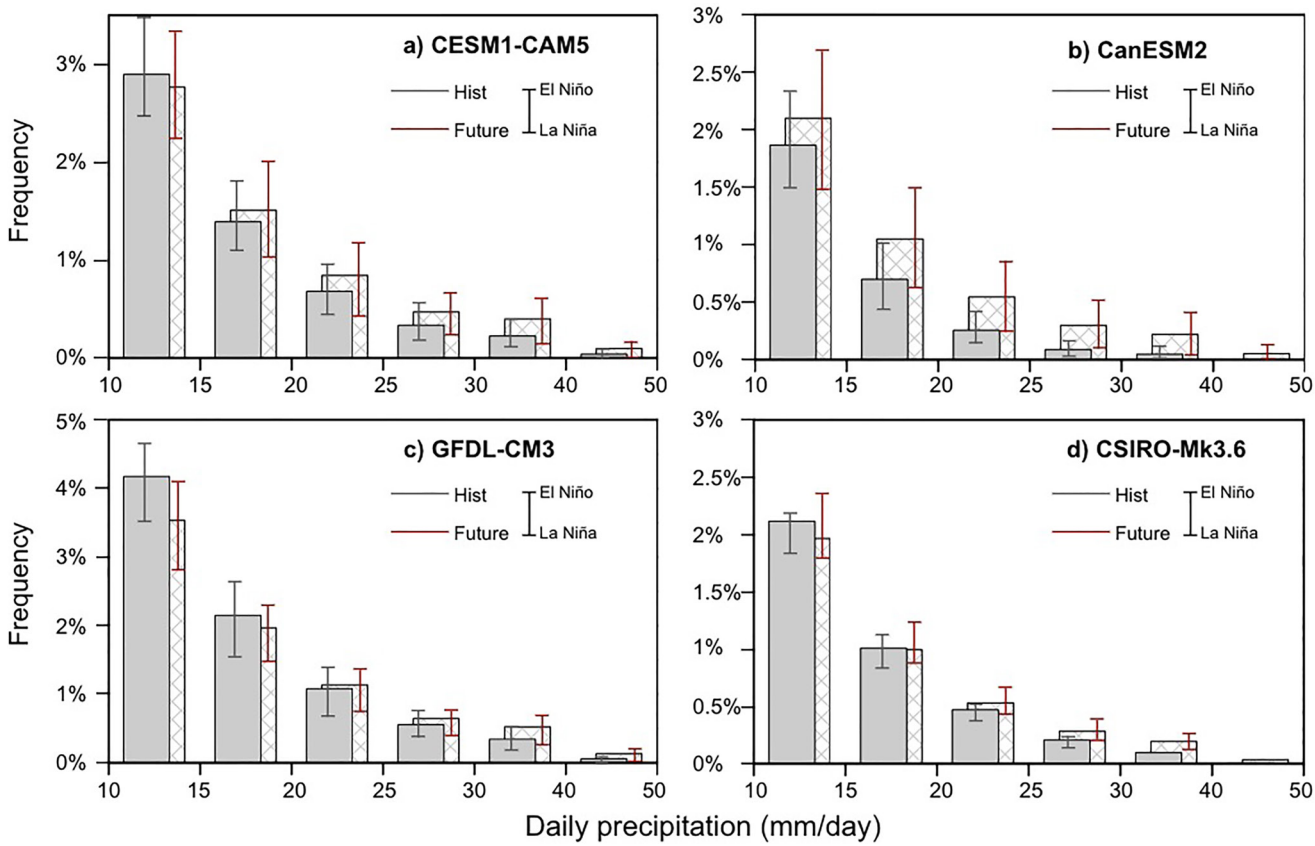

Figure 4. Daily precipitation distributions and their relationship with El Niño/Southern Oscillation (ENSO) phases, for historical and future climate. Gray and white boxes show the total daily frequency distribution over the historical and future period respectively. The impact of ENSO phases is indicated by the gray and red error bars on the frequency distribution over the historical and future period respectively, where the lower whisker is for the La Niña years (i.e., daily precipitation frequency distribution over La Niña years) and the top whisker is for the El Niño years.

intensity is relatively weaker. This indicates that ENSO representation does have an impact, and that inter-model differences in ENSO behavior are important for improving agreement among projections of future extremes.

To provide a more direct visualization of the relative effects of climate change and ENSO, the statistics of daily precipitation distributions are calculated using all ensemble members, for precipitation amounts ranging from 10 to 50 mm/day (Figure 4). In general, the frequency of heavy precipitation shows larger increases for very intense days in the future period, consistent with a change in the upper tail of the precipitation distribution (most notable above 25 mm/day). The ENSO effects are shown in Figure 4 as the spread between whiskers on each histogram box; the future period generally presents a stronger ENSO impact on the most extreme precipitation values, as indicated by a wider spread between whiskers (indicating difference between El Niño and La Niña phases) relative to the mean frequency. An exception to this rule is the CSIRO-Mk3.6. This may be a result of the CSIRO-Mk3.6's limited ability to accurately represent the ENSO-related SST anomaly pattern. The ENSO related variability of extreme precipitation frequency above 10 mm/day is comparable to the mean values in CESM1 and CanESM2, which is relatively weaker in GFDL-CM3 and CSIRO-Mk3.6. This implies that the effect of ENSO variability on the distribution of precipitation can be comparable to the effect of climate change - with even larger impacts on very extreme events.

4. Summary and Discussions

In this study, the effect of teleconnections from the El Niño/Southern Oscillation (ENSO) on regional projected precipitation changes over California has been investigated using a combination of large ensemble simulations from the Multi-Model Large Ensemble Archive, and the CMIP5 collection of future projections. Our results show that both external climate forcing and large-scale modes of internal climate variability can affect the occurrence and strength of extreme precipitation events in California.

We investigate how ENSO and its teleconnections affect the future behavior of precipitation extremes. In the MMLEA, the CESM1 is the only model showing significant ENSO strengthening, and CanESM2 the only model where ENSO weakens significantly. The CMIP5 is roughly evenly split on the direction of ENSO amplitude changes with the mean blurring together models with very different behaviors. Despite these differences in projected ENSO amplitude, there appear to be some consistent changes in the impact of ENSO on future precipitation extremes. The results show that the fraction of extreme precipitation days occurring during El Niño years increases in the future for all models. Further, precipitation extremes are predicted to be nearly the same or less frequent during La Niña years in all models.

In both El Niño and La Niña years, the ensemble spread is quite large, in some cases comparable to the climate change signal - this implies that internal variability contributes strongly to the ENSO impact on precipitation extremes. However, the distinct behaviors of the MMLEA ensembles also demonstrate that inter-model differences in ENSO behavior are important for improving agreement among projections of future extremes. The ENSO influence is particularly apparent for the most extreme precipitation values, and in fact the difference between El Niño and La Niña years is even larger than the overall difference between the historical and future periods in some models. We acknowledge that the statistics for the mean and extreme precipitation for CA statewide are not aimed for use in water resource planners at the watersheds' level, constrained by the resolution of the available climate models simulations.

In sum, this work implies that ENSO has a notable influence on modulating the statistics of precipitation extremes over California, both in the historical period and in terms of projected future changes. Our findings also imply that the ENSO influence is associated with inter-model differences and how the model represents ENSO teleconnections. It remains important to better constrain future changes to ENSO-related SSTA patterns and the associated teleconnections, for more accurate projections of future California precipitation extremes.

Conflict of Interest

The authors declare no conflicts of interest relevant to this study.

Data Availability Statement

Data from the MMLEA is publicly accessible via the NCAR Climate Data Gateway (https://www.earthsystemgrid.org/dataset/ucar.cgd.ccsm4.CLIVAR_LE.html). CMIP5 models used in the study are listed in Table S2 in Supporting Information S1. The CMIP5 data is at: https://esgf-node.llnl.gov/search/cmip5/, CPC Unified Gauge-Based Analysis of Daily Precipitation is from: https://psl.noaa.gov/data/gridded/data.cpc.globalprecip.html, and NCEP reanalysis data is from: https://psl.noaa.gov/data/reanalysis/reanalysis.shtml. All post-processed data used in this study can be accessed at the online public portal (link: https://portal.nersc.gov/project/m3529/ensopr/).

Acknowledgments
We thank the editor and two anonymous reviewers for their comprehensive comments that helped to improve the manuscript substantially. We acknowledge the Multi-Model Large Ensemble Archive (MMLEA) at the National Center for Atmospheric Research for making multiple climate models' ensemble members readily accessible. We also acknowledge the open-shared data set used in this study including CMIP5 data, CPC and NCEP data. XH and SS were supported by the U.S. Department of Energy, DE-SC0019418.

References

Bellenger, H., Guilyardi, É., Leloup, J., Lengaigne, M., & Vialard, J. (2014). ENSO representation in climate models: From CMIP3 to CMIP5. *Climate Dynamics*, *42*(7), 1999–2018. https://doi.org/10.1007/s00382-013-1783-z

Cayan, D. R., Redmond, K. T., & Riddle, L. G. (1999). ENSO and hydrologic extremes in the western United States. *Journal of Climate*, *12*(9), 2881–2893. https://doi.org/10.1175/1520-0442(1999)012<2881:eaheit>2.0.co;2

Deser, C., Lehner, F., Rodgers, K. B., Ault, T., Delworth, T. L., DiNezio, P. N., et al. (2020). Insights from Earth system model initial-condition large ensembles and future prospects. *Nature Climate Change*, *10*(4), 277–286. https://doi.org/10.1038/s41558-020-0731-2

Dettinger, M. D. (2013). Atmospheric rivers as drought busters on the US West Coast. *Journal of Hydrometeorology*, *14*(6), 1721–1732. https://doi.org/10.1175/jhm-d-13-02.1

Dettinger, M. D., Ralph, F. M., Das, T., Neiman, P. J., & Cayan, D. R. (2011). Atmospheric rivers, floods and the water resources of California. *Water*, *3*(2), 445–478. https://doi.org/10.3390/w3020445

Fredriksen, H. B., Berner, J., Subramanian, A. C., & Capotondi, A. (2020). How does El Niño–Southern Oscillation change under global warming—A first look at CMIP6. *Geophysical Research Letters*, *47*(22), e2020GL090640. https://doi.org/10.1029/2020gl090640

Hoell, A., Hoerling, M., Eischeid, J., Wolter, K., Dole, R., Perlwitz, J., et al. (2016). Does El Niño intensity matter for California precipitation? *Geophysical Research Letters*, *43*(2), 819–825. https://doi.org/10.1002/2015gl067102

Huang, X., & Stevenson, S. (2021). Connections between mean North Pacific circulation and western US precipitation extremes in a warming climate. *Earth's Future*, *9*(6), e2020EF001944. https://doi.org/10.1029/2020ef001944

Huang, X., Stevenson, S., & Hall, A. D. (2020). Future warming and intensification of precipitation extremes: A "double whammy" leading to increasing flood risk in California. *Geophysical Research Letters*, *47*(16), e2020GL088679. https://doi.org/10.1029/2020GL088679

Huang, X., & Swain, D. L. (2022). Climate change is increasing the risk of a California megaflood. *Science Advances*, *8*(31), eabq0995. https://doi.org/10.1126/sciadv.abq0995

Huang, X., Swain, D. L., & Hall, A. D. (2020). Future precipitation increase from very high resolution ensemble downscaling of extreme atmospheric river storms in California. *Science Advances*, *6*(29), eaba1323. https://doi.org/10.1126/sciadv.aba1323

Jong, B. T., Ting, M., & Seager, R. (2016). El Niño's impact on California precipitation: Seasonality, regionality, and El Niño intensity. *Environmental Research Letters*, *11*(5), 054021. https://doi.org/10.1088/1748-9326/11/5/054021

Maher, N., Wills, R. C. J., DiNezio, P., Klavans, J., Milinski, S., Sanchez, S. C., et al. (2022). The future of the El Niño-Southern Oscillation: Using large ensembles to illuminate time-varying responses and inter-model differences. *Earth System Dynamics Discussions*, 1–28.

Oakley, N. S., Cannon, F., Munroe, R., Lancaster, J. T., Gomberg, D., & Ralph, F. M. (2018). Brief communication: Meteorological and climatological conditions associated with the 9 January 2018 post-fire debris flows in Montecito and Carpinteria, California, USA. *Natural Hazards and Earth System Sciences*, *18*(11), 3037–3043. https://doi.org/10.5194/nhess-18-3037-2018

O'Gorman, P. A., & Schneider, T. (2009). The physical basis for increases in precipitation extremes in simulations of 21st-century climate change. *Proceedings of the National Academy of Sciences of the United States of America*, *106*(35), 14773–14777. https://doi.org/10.1073/pnas.0907610106

Okumura, Y. M., & Deser, C. (2010). Asymmetry in the duration of El Niño and La Niña. *Journal of Climate*, *23*(21), 5826–5843. https://doi.org/10.1175/2010jcli3592.1

Payne, A. E., & Magnusdottir, G. (2014). Dynamics of landfalling atmospheric rivers over the North Pacific in 30 years of MERRA reanalysis. *Journal of Climate*, *27*(18), 7133–7150. https://doi.org/10.1175/jcli-d-14-00034.1

Pendergrass, A. G., & Hartmann, D. L. (2014). Changes in the distribution of rain frequency and intensity in response to global warming. *Journal of Climate*, *27*(22), 8372–8383. https://doi.org/10.1175/jcli-d-14-00183.1

Pfahl, S., O'Gorman, P. A., & Fischer, E. M. (2017). Understanding the regional pattern of projected future changes in extreme precipitation. *Nature Climate Change*, *7*(6), 423–427. https://doi.org/10.1038/nclimate3287

Ralph, F. M., Neiman, P. J., & Wick, G. A. (2004). Satellite and CALJET aircraft observations of atmospheric rivers over the eastern North Pacific Ocean during the winter of 1997/98. *Monthly Weather Review*, *132*(7), 1721–1745. https://doi.org/10.1175/1520-0493(2004)132<1721:sacaoo>2.0.co;2

Rupp, D. E., Abatzoglou, J. T., Hegewisch, K. C., & Mote, P. W. (2013). Evaluation of CMIP5 20th century climate simulations for the Pacific Northwest USA. *Journal of Geophysical Research: Atmospheres*, *118*(19), 10884–10906. https://doi.org/10.1002/jgrd.50843

Schubert, S. D., Chang, Y., Suarez, M. J., & Pegion, P. J. (2008). ENSO and wintertime extreme precipitation events over the contiguous United States. *Journal of Climate*, *21*(1), 22–39. https://doi.org/10.1175/2007jcli1705.1

Simpson, I. R., Shaw, T. A., & Seager, R. (2014). A diagnosis of the seasonally and longitudinally varying midlatitude circulation response to global warming. *Journal of the Atmospheric Sciences*, *71*(7), 2489–2515. https://doi.org/10.1175/jas-d-13-0325.1

Stevenson, S., Wittenberg, A. T., Fasullo, J., Coats, S., & Otto-Bliesner, B. (2021). Understanding diverse model projections of future extreme El Niño. *Journal of Climate*, *34*(2), 449–464. https://doi.org/10.1175/jcli-d-19-0969.1

Stevenson, S. L. (2012). Significant changes to ENSO strength and impacts in the twenty-first century: Results from CMIP5. *Geophysical Research Letters*, *39*(17). https://doi.org/10.1029/2012gl052759

Taylor, K. E., Stouffer, R. J., & Meehl, G. A. (2012). An overview of CMIP5 and the experiment design. *Bulletin of the American Meteorological Society*, *93*(4), 485–498. https://doi.org/10.1175/bams-d-11-00094.1

White, A. B., Moore, B. J., Gottas, D. J., & Neiman, P. J. (2019). Winter storm conditions leading to excessive runoff above California's Oroville Dam during January and February 2017. *Bulletin of the American Meteorological Society*, *100*(1), 55–70. https://doi.org/10.1175/bams-d-18-0091.1

Zhu, Y., & Newell, R. E. (1998). A proposed algorithm for moisture fluxes from atmospheric rivers. *Monthly Weather Review*, *126*(3), 725–735. https://doi.org/10.1175/1520-0493(1998)126<0725:apafmf>2.0.co;2

References From the Supporting Information

Hawkins, E., Smith, R. S., Gregory, J. M., & Stainforth, D. A. (2016). Irreducible uncertainty in near-term climate projections. *Climate Dynamics*, *46*(11–12), 3807–3819. https://doi.org/10.1007/s00382-015-2806-8

Jeffrey, S., Rotstayn, L., Collier, M., Dravitzki, S., Hamalainen, C., Moeseneder, C., et al. (2013). Australia's CMIP5 submission using the CSIRO-Mk3. 6 model. *Australian Meteorological and Oceanographic Journal*, *63*(1), 1–13. https://doi.org/10.22499/2.6301.001

Kay, J. E., Deser, C., Phillips, A., Mai, A., Hannay, C., Strand, G., et al. (2015). The community Earth system model (CESM) large ensemble project: A community resource for studying climate change in the presence of internal climate variability. *Bulletin of the American Meteorological Society*, *96*(8), 1333–1349. https://doi.org/10.1175/BAMS-D-13-00255.1

Kirchmeier-Young, M. C., Zwiers, F. W., & Gillett, N. P. (2017). Attribution of extreme events in Arctic sea ice extent. *Journal of Climate*, *30*(2), 553–571.

Planton, Y. Y., Guilyardi, E., Wittenberg, A. T., Lee, J., Gleckler, P. J., Bayr, T., et al. (2021). Evaluating climate models with the CLIVAR 2020 ENSO metrics package. *Bulletin of the American Meteorological Society*, *102*(2), E193–E217. https://doi.org/10.1175/bams-d-19-0337.1

Sheffield, J., Barrett, A. P., Colle, B., Nelun Fernando, D., Fu, R., Geil, K. L., et al. (2013). North American climate in CMIP5 experiments. Part I: Evaluation of historical simulations of continental and regional climatology. *Journal of Climate*, *26*(23), 9209–9245. https://doi.org/10.1175/JCLI-D-12-00592.1

Sun, L., Alexander, M., & Deser, C. (2018). Evolution of the global coupled climate response to Arctic sea ice loss during 1990–2090 and its contribution to climate change. *Journal of Climate*, *31*(19), 7823–7843. https://doi.org/10.1175/jcli-d-18-0134.1